


Emblems of pair density waves: Dual identity of topological defects and their transport signaturesOmri Lesser¹, Chunli Huang², James P. Sethna¹, and Eun-Ah Kim^{1,3}¹*Department of Physics, Cornell University, Ithaca, New York 14853, USA*²*Department of Physics and Astronomy, University of Kentucky, Lexington, Kentucky 40506-0055, USA*³*Department of Physics, Ewha Womans University, Seoul, South Korea* (Received 14 June 2025; revised 17 December 2025; accepted 12 May 2026; published 1 June 2026)

The pair density wave (PDW) exemplifies intertwined orders in strongly correlated systems. A recent discovery of superconductivity in a quarter-metal state [T. Han *et al.*, *Nature (London)* **643**, 654 (2025)] offers the first experimental system where a pure PDW without uniform superconductivity is suspected, offering a unique opportunity to examine the consequences of intertwined orders. A pure two-dimensional PDW supports an unusual fractional excitation as its topological defect (TD). A TD simultaneously winds the phase of the Cooper pair and distorts the amplitude modulation—a dual role reflecting its intertwined character. As a vortex, a TD carries fractional vorticity of $\frac{1}{3}h/2e$, whose movement would cause resistance. As a crystalline defect, a TD can be sourced by charge disorder in the system. We show that experimentally observed resistive switching can originate from mobile TDs, while a small magnetic field will restore zero resistance by blocking their motion. The resulting resistive state exhibits extreme anisotropy and a Hall response, with the Hall angle determined by the angle between the current and the TD's Burgers vector. These features will serve as confirmation of the dual identity of topological defects as emblems of PDW order.

DOI: [10.1103/PhysRevB.113.214505](https://doi.org/10.1103/PhysRevB.113.214505)**I. INTRODUCTION**

Ever since intriguing transport observations in cuprate superconductors invited the invocation of the concept [1,2], the notion of a pair density wave (PDW), a finite-momentum carrying paired state, has become a fixture in studies of strongly correlated superconductors such as cuprates [3–7], UTe_2 [8,9], kagome materials [10–14], and transition metal dichalcogenides [15,16]. PDWs in such strongly correlated systems are anticipated without a magnetic field breaking spin degeneracy, unlike in early proposals by Fulde and Ferrell (FF) [17] or Larkin and Ovchinnikov (LO) [18]. Hence, their existence signals strong correlation driving physics beyond the Fermi-surface instability and garnered much interest. However, the candidate systems thus far all contained charge density wave order and a uniform superconducting component. The fact that the modulated component's amplitude is subdominant incurred the criticism of the PDW being a subsidiary effect. Practically, such subdominance also meant many of the interesting properties of PDWs have been hard to resolve.

An intriguing recent experiment on rhombohedral tetralayer graphene [19] invites us to think about pure PDW order (see also Ref. [20] for another experiment on a similar platform). In the experiment, superconductivity was reported in a two-dimensional material with the parent state being a spin- and valley-polarized quarter metal; see Fig. 1(a). In such a state, superconducting pairing must take place *within* a valley, leading to finite Cooper pair momentum: pure PDW, without a uniform component, is natural [21]. If confirmed, this will be the first case of a pure PDW which must have a very unusual mechanism. Several theoretical works have considered the possible mechanisms and order parameter symmetries in this unusual superconductor [22–34]. However, the connection between

the observations and the PDW nature remains unclear. Much needed is strong evidence supporting the PDW nature that goes beyond the normal-state circumstances.

The phenomenology observed in Ref. [19] is mostly in line with conventional superconductivity, except for one significant departure depicted in Fig. 1(b) (adapted from Ref. [19]): the zero-field resistance exhibits temporal switching behavior (telegraph noise) [35]. This behavior, unique to the phase labeled SC1 in Ref. [19], is the main subject of this paper, as a potential harbinger of the pair density wave order. In what follows, we will argue that topological defects in the PDW order can explain the switching behavior shown in Fig. 1(b). The key realization is that defects in a multicomponent PDW have a dual identity: the Cooper pair phase winds around a topological defect (TD) [see Fig. 1(c)], which is simultaneously a 5-7 pair crystalline dislocation [see Fig. 1(d)]. The physics of vortices and that of crystalline dislocations are individually well studied. The proliferation of vortices in two-dimensional superconductors leads to the destruction of quasi-long-range order via the Berezinskii-Kosterlitz-Thouless mechanism [36,37], and in two-dimensional crystals, the proliferation of structural defects leads to melting [38–40]. Here, we study the formation of TDs in pairs at nucleation centers—defects or soft spots in the superconducting order (see Fig. 3). Nucleation is dominated by defects (e.g., dust grains nucleating raindrops in water vapor stressed by supercooling); nucleation of TDs at defects allows for the local release of the stresses [e.g., Frank-Read sources [41] nucleating slip through the release of a periodic array of three-dimensional (3D) dislocations under shear stress [42–44]]. Current will impose stress on the superconducting vortex component of our defects, mediating a continuous stream of TDs causing the observed resistance jumps.

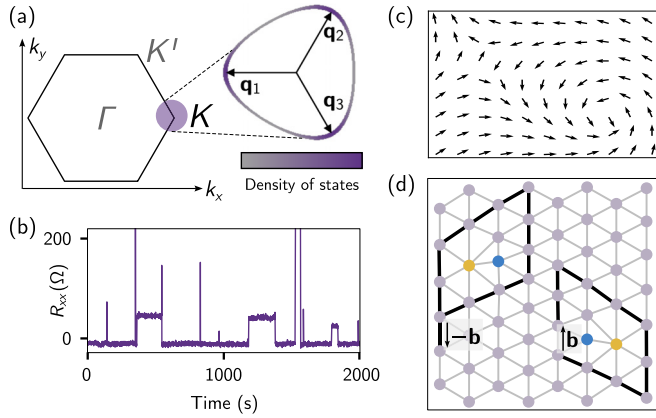


FIG. 1. (a) The Brillouin zone of (multilayer) graphene. In the quarter-metal phase, only one of the valleys (K in this illustration) is occupied. The Fermi surface around K is trigonally warped, leading to three hot spots with a high density of states, denoted by the momenta \mathbf{q}_1 , \mathbf{q}_2 , \mathbf{q}_3 . (b) Experimental data from Ref. [19] showing time-dependent resistance fluctuations in one of the superconducting states of rhombohedral tetralayer graphene. (c) Illustration of the phase of an ordinary two-dimensional superconductor with a vortex and an antivortex. (d) 5 (blue)-7 (yellow) pair crystalline defect of a triangular lattice. The loops around the defects show the Burgers vector \mathbf{b} .

II. PAIR DENSITY WAVES WITH TOPOLOGICAL DEFECTS

We begin by describing the long-range ordered PDW pattern without TDs. As indicated in Fig. 1(a), trigonal warping induces three hot spots in the Fermi surfaces, with momenta \mathbf{q}_1 , \mathbf{q}_2 , \mathbf{q}_3 relative to the K point. The most natural form of spatial modulation is of the FF type (phase modulation). The

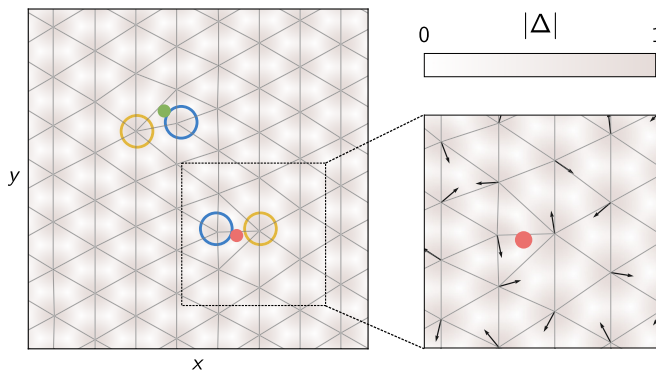


FIG. 2. The PDW and its TDs, calculated using Eq. (1). The color scale indicates the PDW order parameter's magnitude, whereas the arrows correspond to its phase. The three phase-modulated components lead to both amplitude and phase modulations, with the amplitude maxima defining an emergent triangular lattice. The 5 (yellow)-7 (blue) crystalline defect pairs are TDs with $\pm\frac{1}{3}$ flux quantum attached due to 2π winding of only one of the three components of the order parameter.

overall pairing order parameter in this case is

$$\Delta(\mathbf{r}) = \sum_{j=1}^3 \Delta_{\mathbf{q}_j} e^{i(2\mathbf{K}+\mathbf{q}_j)\cdot\mathbf{r}}, \quad (1)$$

where $\{\Delta_{\mathbf{q}_j}\}$ are the three order parameters corresponding to the three modulation vectors $\{\mathbf{q}_j\}$ [45] that are incommensurate with the underlying lattice, leading to $U(1) \times U(1) \times U(1)$ symmetry. In the C_3 symmetric case, the $\{\Delta_{\mathbf{q}_j}\}$ are all equal, resulting in the modulation pattern shown in Fig. 2; see also Refs. [46,47]. Due to the three-component structure of the PDW, the pure FF phase modulation now also has a LO (amplitude) component (see Fig. 2), forming a honeycomb lattice of vortices and antivortices. This crystal of Cooper pairs can be viewed as an antiferromagnetic lattice of vortices, and it forms the background upon which we will now study topological defects. This emergent crystal will be pinned by charge disorder, keeping vortices frozen in place without causing resistance.

As was first noted in Refs. [1,2,48], unlike conventional superconductors, unidirectional PDWs with a two-component order parameter $\Delta(\mathbf{r}) = (\Delta_{\mathbf{Q}}, \Delta_{-\mathbf{Q}}) \propto (e^{i\phi_1}, e^{i\phi_2})$ support half-quantum vortices where a single phase ϕ_1 or ϕ_2 winds by 2π , yielding a magnetic flux of $h/4e$. The consistency of these half-quantum vortices with a single-valued wave function is ensured by their composite nature, where a π phase winding in the superconducting order is accompanied by a half dislocation in the periodic PDW structure. This is similar to the way half-quantum vortices are allowed in spin-triplet superconductors, where single-valuedness of the superconducting order parameter is guaranteed by phase winding in the spin degree of freedom, making up for half vorticity [48,49]. In our case, the presence of three order parameters leads to an analogous “ $\frac{1}{3}$ vortex” as the lowest-energy defect (see Sec. SI of the Supplemental Material [50] and Refs. [51,52] therein). Figure 2 shows a pair of such fractional vortices, introduced by winding only Δ_1 of Eq. (1) (we notice that winding in Δ_2 or Δ_3 is equally valid due to the C_3 symmetry). It is evident that, besides their vortex nature, these defects are also dislocations of the triangular lattice, known as 5-7 pairs [36,39,53–56]: in the pristine triangular lattice each site has six neighbors, and the defects distort the lattice such that one site has five neighbors and another has seven. A unique feature of our three-component PDW is that it enables a magnetic object—the $\pm\frac{1}{3}$ vortex—to be sourced and pinned by charge impurities, through its dual role as a crystalline defect. This unusual possibility of charge impurities sourcing a fractional vortex-antivortex pair, $\{\frac{1}{3}, -\frac{1}{3}\}$, without an external magnetic field, reflects the crux of the intertwined nature of the PDW.

Having identified the elementary topological defects, we now discuss their motion and its relation to resistance. Due to the amplitude modulation of the pairing order parameter, a weak spot (caused by a charge impurity) can serve as a source of TD-anti-TD pair [41] at zero magnetic field, as illustrated in Figs. 3(a)–3(d). When a current \mathbf{J} is applied in the \hat{x} direction, the TDs and anti-TDs move in the $\pm\hat{y}$ direction, respectively, due to the Lorentz force acting on them by virtue of their nature as $\pm\frac{1}{3}$ vortices. Within the Bardeen-Stephen theory [57], this force is balanced by a viscous force $-\eta\mathbf{v}$, leading to a constant terminal velocity

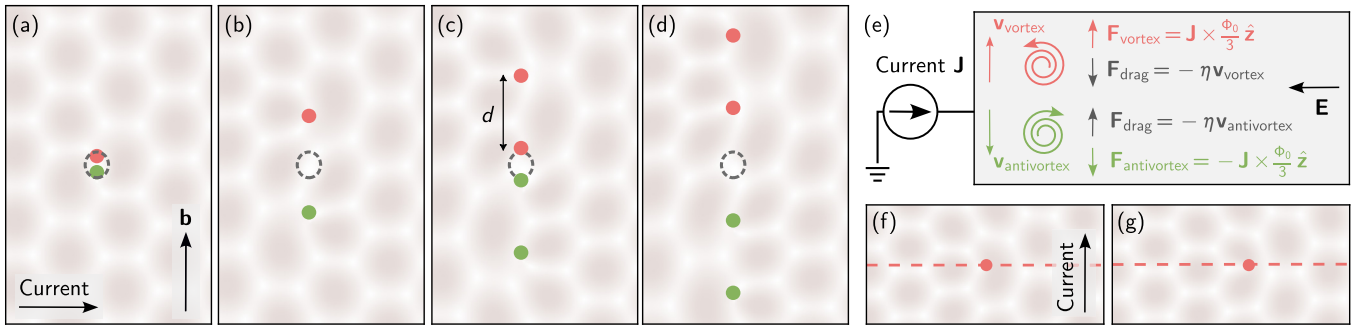


FIG. 3. The motion of defects in the pair density wave background and its associated resistance. (a), (b) A weak spot in the superconductor (dashed circle) becomes a constant source of defect-antidefect pairs. Current makes the defects (red) and antidefects (green) move in opposite directions. The Burgers vector $\mathbf{b} = b\hat{\mathbf{y}}$ associated with the defects is vertical. (c), (d) When the defects get far enough from the source, a second pair of defects leaves it and starts moving with the same velocity. (e) Bardeen-Stephen mechanism for resistance due to vortex motion. The horizontal current \mathbf{J} induces a Lorentz force on the $\pm \frac{1}{3}$ vortices, making them move in opposite directions, and the viscosity η determines their terminal velocity. The motion of fluxes causes an electric field $\mathbf{E} \propto -\mathbf{v}_{\text{vortex}} \times \frac{\Phi_0}{3} \hat{\mathbf{z}}$ in the horizontal direction, which leads to a voltage drop and hence to resistance. (f), (g) The background landscape of modulated superconductivity makes it harder for a defect to climb in the horizontal direction (dashed line) compared to gliding in the vertical motion shown in (a)–(d).

of the defects. Since defects of the same topological charge logarithmically repel each other, the TD and anti-TD both must travel some distance d from the charge-impurity source before a new pair of defects is generated. We therefore get a steady flow of defects along the vertical direction, leading to a voltage buildup in the horizontal direction, as depicted in Fig. 3(e).

Within the Bardeen-Stephen theory [57], the resistance due to a single mobile vortex is $R = \Phi_0^2 / (\eta L_x L_y)$, where L_x, L_y are the physical dimensions of the system and $\Phi_0 = h/2e$. For a field-induced full vortex whose superconducting order parameter is completely suppressed at its core, the viscosity is phenomenologically estimated to be $\eta_0 = \Phi_0^2 / (2\pi \xi^2 R_N)$, where R_N is the normal-state resistance and ξ is the SC coherence length (see Sec. SII of the Supplemental Material [50]). This result hinges on the assumption that the vortex core is completely metallic with resistance R_N and that its radius is ξ . For the tetralayer graphene of interest [19], the situation is very different: as only one of the three components vanishes at the core of our TDs, we anticipate the effective viscosity η_{eff} for the TDs to be different from what one expects from the normal-state resistance. Furthermore, the core size need not be ξ as it is for standard vortices. In the absence of microscopic details, it is therefore hard to predict the values of the resistance plateaus shown in Fig. 1(b) and their duration. In fact, the underlying reason for the duration of the plateaus is hard to determine even in classic telegraph noise settings in nanostructures [35], and therefore we cannot make any claim regarding its origin in Ref. [19].

We can, however, propose a microscopic mechanism that accounts for the resistive plateaus observed in Ref. [19] and illustrated in Fig. 1(b). Thermal fluctuations can cause weak spots in the sample to couple to the SC order and become sources of defect pairs. Once the TDs are created, they start moving due to the current, and generate resistance as per the Bardeen-Stephen theory [57] (see Sec. SII of the Supplemental Material [50] for an elaboration). Their motion is along a vertical line [see Figs. 3(a)–3(d)]. When a TD reaches the edge it disappears, since the lattice sites near the edge do

support 5-7 dislocations (their coordination number is lower than 6 anyway). However, the source keeps generating mobile TDs, and therefore the resistance maintains its steady-state value. The almost instantaneous onset of the resistive plateaus in Fig. 1(b) suggests that the system quickly reaches the steady state, where L_y/d defects are moving along the line. Indeed, for any reasonable estimate of the velocity of the TDs (see Sec. SII of the Supplemental Material [50]), the timescale for reaching the steady state is < 200 ms, much shorter than the duration of the plateau (hundreds of seconds). Finally, the zero-resistance state can be restored by another random thermal event, which leads to a reconfiguration of the impurities in such a way that the defect source is turned off. When that happens, the remaining defects will make their way to the edge and quickly disappear, explaining the apparent abrupt vanishing of the resistive state.

The dual identity of the TDs will manifest through extreme anisotropy in the above resistance resulting from the TD motion. The movement of dislocations in crystals requires bond switching events [58] making it much easier for the dislocations to glide than climb. This aspect of crystalline defects gained new interest from the perspective of so-called *lineons* [56]: emergent particles whose motion is restricted to a lower-dimensional subspace of the space that supports the particle. Given that our TDs are defined atop an emergent “crystal” of PDW, the anisotropy may not be so severe as to prevent motion along one direction. Nonetheless, clearly distinct deformations required by the glide shown in Figs. 3(a)–3(d) and climb shown in Figs. 3(f) and 3(g) would imply strong directional anisotropy in electrical transport that could provide an experimental signature of these exotic excitations.

III. APPLYING AN EXTERNAL MAGNETIC FIELD

We now turn our attention to the fate of the resistance fluctuations under an external out-of-plane magnetic field B_{\perp} . B_{\perp} will introduce external vortices. Each vortex will suppress the superconducting amplitude at its core and erase the emergent PDW “lattice site” to introduce a vacancy, as illustrated for a

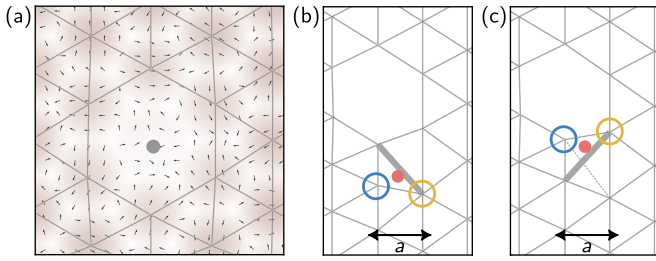


FIG. 4. The effect of an external magnetic field B_{\perp} on defects. (a) A field-induced vortex suppressing the pair amplitude and creating a vacancy, illustrated for the case of vortex creation at the local pair amplitude maximum. (b), (c) A TD (red dot) associated with the 5-7 defect (blue and yellow circles) moves through a bond (thick gray line) switching among the lattice sites. A vacancy will present a roadblock for defects within a strip of width a (the lattice separation).

simple case of a vortex landing on a local peak of superconducting pair amplitude in Fig. 4(a) [59]. Since a TD moves by switching bonds [see Figs. 4(b) and 4(c)], introducing a vacancy through a field-induced vortex on the preferred path of TD's motion will hinder the TD motion. For the TD to move, it must circumvent the vacancy by departing from its preferred direction of movement. On the other hand, a vacancy at locations away from the preferred path of motion will not affect the TD motion. Assuming that the vortex has to land within the PDW lattice constant a around the preferred path of TD, the likelihood that a vortex will disrupt the TD motion at low field is small if vortex could land anywhere in the sample of width L_x . However, upon increasing the external field B_{\perp} which introduces more and more full vortices, it will become more likely for one of those vortices to present a roadblock and stop the movement of TDs, halting the steady flow and generation of TDs. Hence the system will lose the telegraph noise such as the occurrence of resistive states at a threshold value of perpendicular magnetic field B_{\perp} .

For a ballpark estimate of the requisite field strength, we consider the external vortex to be equally likely to land anywhere on the sample. Then the probability of at least one of them being within the strip of width a of the preferred path is $p = 1 - (1 - a/L_x)^{N_v}$, where $N_v = [\Phi_0/(B_{\perp}L_xL_y)]$ is the number of vortices ($[x]$ means rounding x to the nearest integer). For the tetralayer graphene in Ref. [19], the resistance fluctuations disappear at $B_{\perp} \approx 8$ mT, corresponding to $N_v \approx 108$ vortices (see Sec. SII of the Supplemental Material [50]). With the PDW lattice constant of $a \approx 60$ nm estimated in Ref. [47] and $L_x = 9.6 \mu\text{m}$, the blocking probability is roughly $p = 0.1$ at the threshold field strength, which appears to be a reasonable likelihood for the blockage to occur.

IV. CONCLUSION

Taking a step back and analyzing our results, it is crucial to identify the main physical origins and consequences of the PDW order. The periodic, crystal-like structure formed by the PDW alone cannot explain the observed resistive behavior; despite containing many vortices and antivortices [47], these are not free to move and therefore cannot generate resistance.

Since mobile vortices are the only plausible mechanism for finite resistance in a superconductor, the observation of such behavior at zero magnetic field is highly unusual. In standard superconductors, even when magnetic fields are present, pinning effects typically immobilize vortices. Therefore, the key requirement is a crystal whose defects have dual facets: they function as vortices, causing resistance when mobile, while simultaneously acting as crystalline defects that couple to charge disorder and occur naturally in two-dimensional crystals. This dual identity of the defects manifests the most salient property of PDWs: the coupling between positional modulation and the superconducting phase, which is conjugate to the Cooper pair number. We emphasize that the defects discussed here are topological defects of the emergent PDW crystal itself, not microscopic impurities in the underlying lattice. The multicomponent PDW brings in precisely the necessary elements, and our subsequent analysis of resistive behavior follows from simple physical considerations. While we do not claim this is the only possible explanation for the observations reported in Ref. [19], reconciling superconductivity, resistive jumps, and a quarter-metal normal state through alternative mechanisms presents significant challenges.

Our theoretical analysis, combined with the experimental results [19], opens several avenues for future research. The restricted mobility of the defects could be directly tested experimentally by driving current in two perpendicular directions and comparing the resulting resistance values. We anticipate strong anisotropy in these measurements, as the triangular lattice structure inherently prevents both directions from being allowed. Another prediction of our theory is that, if the current is not perpendicular to the Burgers vector but rather oriented at some angle θ with respect to it (here, $\theta = \pm 60^\circ$), then a Hall voltage will be induced due to the defects' motion, with Hall angle $R_{xy}/R_{xx} = \cot \theta$ (see Sec. SIII of the SM). Such a confirmation would position multicomponent PDWs as the first genuine experimental realization of lineon dynamics in condensed matter systems. Moreover, the findings provide compelling motivation for further investigations into the properties of pure PDWs. Particularly intriguing are the nature of bound states in $\frac{1}{3}$ vortices and their implications for measurable properties, which remain largely unexplored.

ACKNOWLEDGMENTS

We are grateful to S. A. Kivelson and M. Rosales for insightful discussions. We thank L. Ju and T. Han for sharing their experimental data with us. We thank D. F. Agterberg, Y. Wang, R. Thomale, and P. A. Lee for useful comments on the manuscript. This research was supported in part by grant NSF PHY-2309135 to the Kavli Institute for Theoretical Physics (KITP). O.L. is supported by a Bethe-KIC postdoctoral fellowship at Cornell University. O.L. and E.-A.K. are supported by the U.S. Department of Energy through Award No. DE-SC0023905. J.P.S. is supported by NSF DMR-2327094.

DATA AVAILABILITY

The data that support the findings of this article are not publicly available. The data are available from the authors upon reasonable request.

- [1] A. Himeda, T. Kato, and M. Ogata, Stripe states with spatially oscillating d -wave superconductivity in the two-dimensional t - t' - J model, *Phys. Rev. Lett.* **88**, 117001 (2002).
- [2] E. Berg, E. Fradkin, and S. A. Kivelson, Charge- $4e$ superconductivity from pair-density-wave order in certain high-temperature superconductors, *Nat. Phys.* **5**, 830 (2009).
- [3] S. D. Edkins, A. Kostin, K. Fujita, A. P. Mackenzie, H. Eisaki, S. Uchida, S. Sachdev, M. J. Lawler, E.-A. Kim, J. C. S. Davis, and M. H. Hamidian, Magnetic field-induced pair density wave state in the cuprate vortex halo, *Science* **364**, 976 (2019).
- [4] P. Choubey, S. H. Joo, K. Fujita, Z. Du, S. D. Edkins, M. H. Hamidian, H. Eisaki, S. Uchida, A. P. Mackenzie, J. Lee, J. C. S. Davis, and P. J. Hirschfeld, Atomic-scale electronic structure of the cuprate pair density wave state coexisting with superconductivity, *Proc. Natl. Acad. Sci. USA* **117**, 14805 (2020).
- [5] S. Wang, P. Choubey, Y. X. Chong, W. Chen, W. Ren, H. Eisaki, S. Uchida, P. J. Hirschfeld, and J. C. S. Davis, Scattering interference signature of a pair density wave state in the cuprate pseudogap phase, *Nat. Commun.* **12**, 6087 (2021).
- [6] Z. Dai, Y.-H. Zhang, T. Senthil, and P. A. Lee, Pair-density waves, charge-density waves, and vortices in high- T_c cuprates, *Phys. Rev. B* **97**, 174511 (2018).
- [7] Y.-M. Wu, A. V. Chubukov, Y. Wang, and S. A. Kivelson, Time-reversal symmetry breaking, collective modes, and Raman spectrum in pair-density-wave states, [arXiv:2501.14138](https://arxiv.org/abs/2501.14138).
- [8] Q. Gu, J. P. Carroll, S. Wang, S. Ran, C. Broyles, H. Siddiquee, N. P. Butch, S. R. Saha, J. Paglione, J. C. S. Davis, and X. Liu, Detection of a pair density wave state in UTe_2 , *Nature (London)* **618**, 921 (2023).
- [9] A. Aishwarya, J. May-Mann, A. Almoalem, S. Ran, S. R. Saha, J. Paglione, N. P. Butch, E. Fradkin, and V. Madhavan, Melting of the charge density wave by generation of pairs of topological defects in UTe_2 , *Nat. Phys.* **20**, 964 (2024).
- [10] H. Li, G. Fabbris, A. H. Said, J. P. Sun, Y.-X. Jiang, J.-X. Yin, Y.-Y. Pai, S. Yoon, A. R. Lupini, C. S. Nelson, Q. W. Yin, C. S. Gong, Z. J. Tu, H. C. Lei, J.-G. Cheng, M. Z. Hasan, Z. Wang, B. Yan, R. Thomale, H. N. Lee, and H. Miao, Discovery of conjoined charge density waves in the kagome superconductor CsV_3Sb_5 , *Nat. Commun.* **13**, 6348 (2022).
- [11] H. Deng, H. Qin, G. Liu, T. Yang, R. Fu, Z. Zhang, X. Wu, Z. Wang, Y. Shi, J. Liu, H. Liu, X.-Y. Yan, W. Song, X. Xu, Y. Zhao, M. Yi, G. Xu, H. Hohmann, S. C. Holbæk, M. Dürnagel, *et al.*, Chiral kagome superconductivity modulations with residual Fermi arcs, *Nature (London)* **632**, 775 (2024).
- [12] Y.-M. Wu, R. Thomale, and S. Raghu, Sublattice interference promotes pair density wave order in kagome metals, *Phys. Rev. B* **108**, L081117 (2023).
- [13] T. Schwemmer, H. Hohmann, M. Dürnagel, J. Potten, J. Beyer, S. Rachel, Y.-M. Wu, S. Raghu, T. Müller, W. Hanke, and R. Thomale, Sublattice modulated superconductivity in the kagome Hubbard model, *Phys. Rev. B* **110**, 024501 (2024).
- [14] M. Yao, Y. Wang, D. Wang, J.-X. Yin, and Q.-H. Wang, Self-consistent theory of 2×2 pair density waves in kagome superconductors, *Phys. Rev. B* **111**, 094505 (2025).
- [15] J. Venderley and E.-A. Kim, Evidence of pair-density wave in spin-valley locked systems, *Sci. Adv.* **5**, eaat4698 (2019).
- [16] Y.-M. Wu, Z. Wu, and H. Yao, Pair-density-wave and chiral superconductivity in twisted bilayer transition metal dichalcogenides, *Phys. Rev. Lett.* **130**, 126001 (2023).
- [17] P. Fulde and R. A. Ferrell, Superconductivity in a strong spin-exchange field, *Phys. Rev.* **135**, A550 (1964).
- [18] A. I. Larkin and Y. Ovchinnikov, Inhomogeneous state of superconductors, *Sov. Phys. JETP* **20**, 762 (1965).
- [19] T. Han, Z. Lu, Z. Hadjri, L. Shi, Z. Wu, W. Xu, Y. Yao, A. A. Cotten, O. Sharifi Sedeh, H. Weldeyesus, J. Yang, J. Seo, S. Ye, M. Zhou, H. Liu, G. Shi, Z. Hua, K. Watanabe, T. Taniguchi, P. Xiong, *et al.*, Signatures of chiral superconductivity in rhombohedral graphene, *Nature (London)* **643**, 654 (2025).
- [20] Y. Choi, Y. Choi, M. Valentini, C. L. Patterson, L. F. W. Holleis, O. I. Sheekey, H. Stoyanov, X. Cheng, T. Taniguchi, K. Watanabe, and A. F. Young, Superconductivity and quantized anomalous Hall effect in rhombohedral graphene, *Nature (London)* **639**, 342 (2025).
- [21] Z. Han and S. A. Kivelson, Pair density wave and reentrant superconducting tendencies originating from valley polarization, *Phys. Rev. B* **105**, L100509 (2022).
- [22] Y.-Z. Chou, J. Zhu, and S. Das Sarma, Intravalley spin-polarized superconductivity in rhombohedral tetralayer graphene, *Phys. Rev. B* **111**, 174523 (2025).
- [23] Q. Qin and C. Wu, Chiral finite-momentum superconductivity in the tetralayer graphene, *Chin. Phys. Lett.* **43**, 030708 (2026).
- [24] H. Yang and Y.-H. Zhang, Topological incommensurate Fulde-Ferrell-Larkin-Ovchinnikov superconductor and Bogoliubov Fermi surface in rhombohedral tetra-layer graphene, [arXiv:2411.02503](https://arxiv.org/abs/2411.02503).
- [25] M. Geier, M. Davydova, and L. Fu, Chiral and topological superconductivity in isospin polarized multilayer graphene, [arXiv:2409.13829](https://arxiv.org/abs/2409.13829).
- [26] M. Kim, A. Timmel, L. Ju, and X.-G. Wen, Topological chiral superconductivity beyond pairing in a Fermi liquid, *Phys. Rev. B* **111**, 014508 (2025).
- [27] C. Yoon, T. Xu, Y. Barlas, and F. Zhang, Quarter-metal superconductivity in rhombohedral graphene, *Phys. Rev. Lett.* **136**, 026603 (2026).
- [28] G. Parra-Martínez, A. Jimeno-Pozo, V. T. Phong, H. Sainz-Cruz, D. Kaplan, P. Emanuel, Y. Oreg, P. A. Pantaleon, J. A. Silva-Guillen, and F. Guinea, Band renormalization, quarter metals, and chiral superconductivity in rhombohedral tetralayer graphene, *Phys. Rev. Lett.* **135**, 136503 (2025).
- [29] A. Daido, Y. Yanase, and K. T. Law, Nonreciprocal current-induced zero-resistance state in valley-polarized superconductors, *Phys. Rev. Lett.* **135**, 236001 (2025).
- [30] A. Gil and E. Berg, Charge and pair density waves in a spin and valley-polarized system at a Van-Hove singularity, [arXiv:2504.19321](https://arxiv.org/abs/2504.19321).
- [31] M. Christos, P. M. Bonetti, and M. S. Scheurer, Finite-momentum pairing and superlattice superconductivity in valley-imbalanced rhombohedral graphene, [arXiv:2503.15471](https://arxiv.org/abs/2503.15471).
- [32] Y. Chen, M. S. Scheurer, and C. Schrade, Intrinsic superconducting diode effect and nonreciprocal superconductivity in rhombohedral graphene multilayers, *Phys. Rev. B* **112**, L060505 (2025).
- [33] A. Jahin and S.-Z. Lin, Spontaneous vortex lattice due to orbital magnetization in valley polarized superconductors, [arXiv:2505.22915](https://arxiv.org/abs/2505.22915).
- [34] D. Sedov and M. S. Scheurer, Probing superconductivity with tunneling spectroscopy in rhombohedral graphene, *Phys. Rev. B* **113**, L140503 (2026).

- [35] K. S. Ralls, D. C. Ralph, and R. A. Buhrman, Individual-defect electromigration in metal nanobridges, *Phys. Rev. B* **40**, 11561 (1989).
- [36] J. M. Kosterlitz and D. J. Thouless, Ordering, metastability and phase transitions in two-dimensional systems, *J. Phys. C: Solid State Phys.* **6**, 1181 (1973).
- [37] J. V. Jos, *40 Years of Berezinskii-Kosterlitz-Thouless Theory* (World Scientific, Singapore, 2013).
- [38] D. R. Nelson, Study of melting in two dimensions, *Phys. Rev. B* **18**, 2318 (1978).
- [39] D. R. Nelson and B. I. Halperin, Dislocation-mediated melting in two dimensions, *Phys. Rev. B* **19**, 2457 (1979).
- [40] M. Hayashi, Effects of dislocations on the stiffness of charge density wave, *Physica B* **324**, 82 (2002).
- [41] F. C. Frank and W. T. Read, Multiplication processes for slow moving dislocations, *Phys. Rev.* **79**, 722 (1950).
- [42] A. Nicolas, E. E. Ferrero, K. Martens, and J.-L. Barrat, Deformation and flow of amorphous solids: Insights from elastoplastic models, *Rev. Mod. Phys.* **90**, 045006 (2018).
- [43] M. Baggioli, I. Kriuchevskiy, T. W. Sirk, and A. Zaccone, Plasticity in amorphous solids is mediated by topological defects in the displacement field, *Phys. Rev. Lett.* **127**, 015501 (2021).
- [44] Z. W. Wu, Y. Chen, W.-H. Wang, W. Kob, and L. Xu, Topology of vibrational modes predicts plastic events in glasses, *Nat. Commun.* **14**, 2955 (2023).
- [45] Y. Yerin, S.-L. Drechsler, M. Cuoco, and C. Petrillo, Multiple- q current states in a multicomponent superconducting channel, *J. Phys.: Condens. Matter* **35**, 505601 (2023).
- [46] D. F. Agterberg, M. Geracie, and H. Tsunetsugu, Conventional and charge-six superfluids from melting hexagonal Fulde-Ferrell-Larkin-Ovchinnikov phases in two dimensions, *Phys. Rev. B* **84**, 014513 (2011).
- [47] F. Gaggioli, D. Guerci, and L. Fu, Spontaneous vortex-antivortex lattice and Majorana fermions in rhombohedral graphene, *Phys. Rev. Lett.* **135**, 116001 (2025).
- [48] D. F. Agterberg and H. Tsunetsugu, Dislocations and vortices in pair-density-wave superconductors, *Nat. Phys.* **4**, 639 (2008).
- [49] S. B. Chung, H. Bluhm, and E.-A. Kim, Stability of Half-Quantum Vortices in $p_x + ip_y$ Superconductors, *Phys. Rev. Lett.* **99**, 197002 (2007).
- [50] See Supplemental Material at <http://link.aps.org/supplemental/10.1103/1gyj-r5fr> for the Ginzburg-Landau theory of fractional vortices in a multicomponent pair density wave and detailed Bardeen-Stephen resistance calculations.
- [51] M. Rosales and E. Fradkin, Electronic structure of topological defects in the pair density wave superconductor, *Phys. Rev. B* **110**, 214508 (2024).
- [52] M. Tinkham, *Introduction to Superconductivity*, 2nd ed., International series in pure and applied physics (McGraw-Hill, New York, 1996).
- [53] A. P. Young, Melting and the vector Coulomb gas in two dimensions, *Phys. Rev. B* **19**, 1855 (1979).
- [54] M. Pretko and L. Radzihovsky, Fracton-elasticity duality, *Phys. Rev. Lett.* **120**, 195301 (2018).
- [55] L. Radzihovsky and M. Hermele, Fractons from vector gauge theory, *Phys. Rev. Lett.* **124**, 050402 (2020).
- [56] A. Gromov and L. Radzihovsky, *Colloquium: Fracton matter*, *Rev. Mod. Phys.* **96**, 011001 (2024).
- [57] M. J. Stephen and J. Bardeen, Viscosity of type-II superconductors, *Phys. Rev. Lett.* **14**, 112 (1965).
- [58] A. J. Stone and D. J. Wales, Theoretical studies of icosahedral C_{60} and some related species, *Chem. Phys. Lett.* **128**, 501 (1986).
- [59] A vortex landing at locations away from the emergent lattice site will suppress more lattice sites, albeit more weakly.